

Computational and Statistical Mechanics of Rock–Paper–Scissors

*David Newth*¹

¹CSIRO Centre for Complex Systems Science
CSIRO Marine and Atmospheric Research
Phone: +61 2 624-21744 Fax: +61 2 624-21677
Email: david.newth@csiro.au

Presented at SIRC 2005 - The 17th Annual Colloquium of the Spatial Information Research Centre
University of Otago, Dunedin, New Zealand
November 24th-25th 2005

ABSTRACT

In the game of rock–paper–scissors, the possible player strategies forms a cycle. In a well mixed environment, we find the so called “*survival of the weakest*” phenomena where the least competitive strategy occupies the bulk of the available resources. In this account I will investigate the dynamics of the spatially constrained version of rock–paper–scissors. Using computational mechanics as a method for analysis the behavior of the system, I demonstrate that the game has four distinct sets of dynamics. Analysis of the structure and size of the clusters formed by groups of like players reveals that the change in dynamics is related to the break down of a giant component. At the transition this cluster is self-similar.

Keywords and phrases: Rock–Paper–Scissors, complex system, statistical complexity, percolation, stochastic cellular automata

1 INTRODUCTION

In the children’s game of rock–paper–scissors, each player chooses one of three strategies either rock, paper or scissors. The alternative strategies form a competitive cycle (where rock defeats scissors, scissors defeats paper and paper defeats rock); with no Nash-equilibrium, as with complete knowledge a player can always select a winning strategy (Sigmund 1993). This simple three strategy game is analogous to a number of well studied biological systems including: mating strategies of side-blotched lizards (Sinervo & Linely 1996); overgrowth by marine sessile organisms (Burrows & Hawkins 1998, Buss 1980, Johnson 1997); competition between mutant strains of yeast; cyclic competition amongst outlaw genes; and predation between corals (Johnson 1997). Like many biological systems the organization of such competitive systems arises from two main sources: (1) the nature of the interactions between the biological agents; and (2) constraints imposed by the environment in which the entities are located.

Intense competition between species lead to notions of competitive exclusion that states complete competitors cannot coexist (Harding 1960). In an environment where the niches of two species completely overlap, the species with even the slightest advantage will eventually drive it’s competitors to extinction. Frean and Abraham (2001) were able to illustrate this point for cyclic succession games such as rock–paper–scissors, by characterizing the steady state and mean population dynamics of the well-mixed or mean-field situation. However the inclusion of spatial constraints, where the interactions between players is local rather than global, dramatically changes the dynamics of the system. Given a large enough domain species can become locally extinct, while distantly separated sub-populations continue to persist. As predators are unable to access their prey, global extinction is unlikely (Frean & Abraham 2001).

My interest here is to study the affect that environmental and spatial constraints have on the population dynamics of cyclic games. In particular I am interested in characterizing the population dynamics of the interacting players, the spatial structures formed and their associated critical values and effect these factors have upon an evolving population. While not providing a complete solution to any of these questions, I will however make an initial move toward a possible solution to this problem. The remainder of this paper is organized as follows. In sections 2 and 3 I will outline the system under study and the framework used to analyze it. In particular section 2 provides an overview of the mean-field and lattice versions of rock–paper–scissors. Section 3 outlines the

computational mechanics framework as proposed by Crutchfield (Crutchfield & Feldman 2003). The percolation properties of rock–paper–scissors is investigated in section 4. Finally section 5 provides a discussion of the results and possible future work.

2 Rock–Paper–Scissors

Here I consider a model world containing N , available sites. Each of the sites can be occupied by one of three species, rock, paper, and scissors, which occur in proportions n_r , n_p , and n_s such that $n_r + n_p + n_s = 1$. At each turn of the game, two players are selected from the pool of N players. The first player can replace the second player with a given probability. An individual of species r , can replace an individual of species s with probability P_r , likewise species s player can replace a species p player with P_s and a species p player can replace a species r player with probability P_p . Substituting numerical indices for species labels the generalized mean-field equations for this system are:

$$\frac{d}{dt}n_j = g_j() = n_j[P_j n_{j+1} - P_{j-1} n_{j-1}], \quad (1)$$

where indices are taken modulo 3. The population density of species j at the fixed point is:

$$n_j^* = \frac{P_{j+1}}{\sum_j P_j}, \quad (2)$$

this point illustrates that the population density of a species is not controlled by its own rate of invasion but by the rate of invasion of the species they invade (Fren & Abraham 2001). As Fren and Abraham (2001) have shown, the mean-field solutions demonstrate the *survival of the weakest property*—The highest density component is that which has the most aggressive prey. In a finite population the trajectory of the population densities will tend to overshoot the orbit eventually leading to the extinction of two of the species. Fren and Abraham found that

$$\lambda = \prod \left(\frac{n_j}{n_j^*} \right)^{n_j^*}, \quad (3)$$

was an invariant along the cyclic path, with $\lambda = 1$ when the population are at the fixed point and $\lambda = 0$ when one or more of the populations become extinct. If n_j^{\min} is the minimum value of n_j along the orbit then

$$\left. \frac{\partial n_j^{\min}}{\partial n_j} \right|_{\lambda^*} > 0, \quad (4)$$

so the species with the smallest fixed point density also has the lowest population density along any orbit. If the invasion rates are unequal, then the species with the lowest fixed point population is the population most likely to become extinct. The species that persist are those with the lowest invasion rates.

2.1 Lattice Model

If the game is spatially constrained, by playing it out upon a regular lattice, where invasions are only allowed to occur locally rather than long range, then the dynamics of the game are substantially changed. Here N sites of the model are taken to be sites on a periodic square lattice, where each site interacts with its eight nearest neighbors. At each time step, each player (the first player) chooses one of its eight nearest neighbors (the second player). The game is then played out. Should the first player lose, then it is invaded or replaced by the second player. When the invasion rates are equal, population fluctuations become stabilized and the populations exist as a series of disconnected sub-clusters (figure 1 Left). If the invasion probabilities are uneven then the populations exist as a series of clusters (figure 1 Centre and Right). Should one of the population invasion rates be substantially smaller than the other two then two populations have patchy distributions and the third exists as a moving wave (figure 1 Right). On small grids, finite size effects lead to two of the species becoming extinct.

As can be seen from figure 1, the population dynamics are no longer solely governed by the replacement probabilities and population densities but are also linked to the structure and shape of the cluster of players being invaded. Such invasion processes and others such as the diffusion of a liquid into a porous media; spread of bushfires; species invasion; and invasion processes like the one described above have been studied as invasion percolation processes (Stauffer 1985). From such studies it is known that an invading epidemic process (such as rock replacing a cluster of scissors), is known to be maximally complex, when the cluster being invaded, is highly self-similar. This generally occurs around some critical threshold. However dynamical games such as rock–paper–scissors, go beyond such two dimensional percolation problems, due to the cyclic nature of the game.

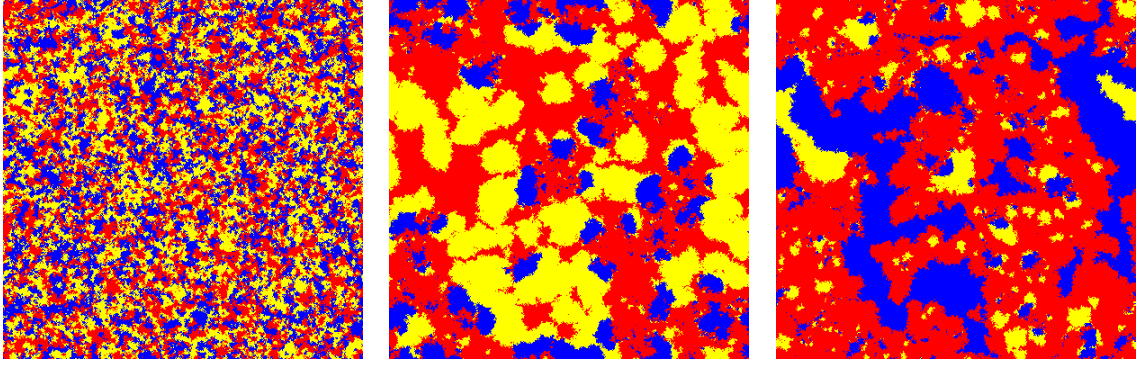


Figure 1: Dynamics rock–paper–scissors with only local interactions on a 500×500 square lattice. (Left) Equal invasion probabilities with $P_0 = 0.\bar{3}$ (Red), $P_1 = 0.\bar{3}$ (Blue) and $P_2 = 0.\bar{3}$ (Yellow). (Centre) Uneven invasion probabilities with $P_0 = 0.05$, $P_1 = 0.5$, $P_2 = 0.5$. (Right) Uneven invasion probabilities $P_0 = 0.1$, $P_1 = 0.1$, $P_2 = 0.8$.

According to Haken (Haken 1998), the emergent properties of a system can be studied via notion of an order parameter, and its associated slaving principle. To simplify the analysis I examine the behavior of the systems by exploring a one-dimensional transect through the space (normalized by $\sum_j P_j = 1$). This was chosen to be $P_0 \in [0, \frac{5}{6}]$, $P_1 = \frac{4}{9} - \frac{P_0}{3}$ and $P_2 = 1 - P_0 - P_1 = \frac{5}{9} - \frac{2P_0}{3}$. In the remainder of this paper, I will examine the population dynamics, cluster structure and evolutionary dynamics of the lattice model of rock–paper–scissors, through the use of computational complexity and percolation theory.

3 Statistical Complexity

Statistical Complexity is a relatively new measure of complexity based on a computational view of the dynamics of a complex system. Statistical complexity has been successfully applied to chaotic dynamical systems (with a period doubling or a quasi-periodic route to chaos, collectives, globally coupled maps (ref), one- and two-dimensional spin systems (ref)). Statistical complexity aims to provide a description of the information content and a computational description of the system under investigation based on its observed behavior. These two complementary views of a system are achieved through an information theoretic analysis of the behavior (which describes the randomness, regularities and uncertainty in the behavior of the system) and a state space reconstruction algorithm (that approximates the computational complexity of the behavior of the system). See (Crutchfield & Feldman 2003) for a full account of this framework. In the remainder of this section I will outline basic framework and measures used to analyze the dynamics of rock–paper–scissors.

3.1 Information Theoretic Framework

In the late 1940's Claude Shannon founded the field of information theory (Shannon 1948). Here I adopt the concept of a communication signal as follows: I assume that there is a *process* (source) that produces a *data stream* (message or signal) —an infinite string of symbols drawn from some finite alphabet \mathcal{A} . The task for the *observer* (receiver) is to estimate the probability distribution of sequences and thereby estimating how random/structured the processes is, and to infer the mechanics of the process creating the stream. The main object of our attention will be a one-dimensional chain $S = \dots s_{-2}, s_{-1}, s_0, s_1, s_2 \dots$ of random variables S_t that range over a discrete finite set \mathcal{A} . The stream S forms a time series that contains information about the properties of the underlying generating process. A block of length L consecutive variables is denoted as $S^L = s_1, \dots, s_L$. I shall use the term process to refer to a joint probability distribution $Pr(S)$ over a finite chain of variables. Shannon referred to such a process as an *information source* (Shannon 1948). Given a signal S from an information source we are interested in determining a number characteristics about the signal including: the diversity of objects within the system, long range correlations between structures, intrinsic memory with the systems, the amount of redundancy within the signal and the irreducible randomness of the signal. The remainder of this section will outline information theoretic statistics for determining these properties.

3.1.1 Block and Source Entropy

The first quantity we are concerned with is the behavior of the Shannon entropy $H(L)$ of $Pr(S^L)$, the distribution over blocks of L consecutive symbols. The total Shannon entropy of length- L sequences is defined as:

$$H(L) = - \sum_{s^L \in \mathcal{A}^L} Pr(s^L) \log_2 Pr(s^L) \quad (5)$$

where $L > 0$. The sum is understood to run over all possible blocks of L consecutive symbols. $H(L)$ measures the uncertainty associated with sequences of length L . The maximum average information per observation of block length- L is $H(L) \leq L \log_2 |\mathcal{A}|$.

The *source entropy rate* $h_\mu(L)$ is the rate of increase of the total entropy with respect to L . In the infinite limit $h_\mu(L)$ is :

$$h_\mu(L) = \lim_{L \rightarrow \infty} \frac{H(L)}{L}. \quad (6)$$

Alternatively, $h_\mu(L)$ can be defined as a finite- L approximation:

$$h_\mu(L) = H(L) - H(L - 1). \quad (7)$$

The source entropy rate $h_\mu(L)$ quantifies the irreducible randomness in observed ensemble of blocks of length- L .

3.1.2 Excess Entropy

Having looked at L -length blocks, an observer can estimate the true randomness h_μ by calculating $h_\mu(L)$, as defined in equation 7. With enough sensory data it can get good approximations to h_μ by using long sequences. But what if there is insufficient data to allow this? To answer this we must determine how the estimates $h_\mu(L)$ converge to h_μ . One measure of convergence is provided by the *excess entropy* E :

$$E = \sum_{L=1}^{\infty} [h_\mu(L) - h_\mu]. \quad (8)$$

E measures the convergence of $h_\mu(L)$ and plays a role in determining how an agent comes to know how random its environment is. But what exactly does E measure? The length- L approximation $h_\mu(L)$ overestimates the entropy rate h_μ at finite L by an amount $h_\mu(L) - h_\mu$. This difference measures how much more random single measurements appear using the finite L -block statistics than the statistics of infinite sequences. In other words, this excess randomness tells us how much additional information must be gained from the environment in order to reveal the actual per-symbol uncertainty h_μ . The excess entropy E , is the total amount of this redundancy and, as such, a measure of one type of memory intrinsic to the environment.

3.1.3 Redundancy

The proportion of information in the L -blocks which is not actually random, but is due to correlations is known as redundancy. Redundancy $R(L)$ can be measured as the information gain or distance between an observed distribution and a uniform distribution. The information gain D between two distributions $Pr(x)$ and $\widehat{Pr}(x)$, is defined as:

$$D = [Pr(x) || \widehat{Pr}(x)] = \sum_{x \in X} \log_2 \frac{Pr(x)}{\widehat{Pr}(x)}, \quad (9)$$

redundancy $R(L)$ is therefore

$$R(L) = \frac{D[Pr(s^L) || U(s^L)]}{L}, \quad (10)$$

where $U(s^L)$ is a uniform distribution, where every block of symbols of length L has occurs with equal probability, i.e. $U(s^L) = \frac{1}{|\mathcal{A}|^L}$. In simple terms $R(L)$ is a measure of the information gain, when an observer expecting a uniform distribution learns the actual distribution over the sequence of symbols.

3.2 ϵ -machine

The aforementioned information quantities have been widely used in the characterization of macroscopic properties and long range correlations in complex systems including cellular automata (ref), spin systems (Crutchfield & Young 1989), genomic data, and weather patterns (ref). As a way of quantifying complexity, it has been shown that these information statistics are appropriate measures of the amount of memory stored by the system (correlations), and they tend to maximize close to critical points. The amount of memory stored by the system is only

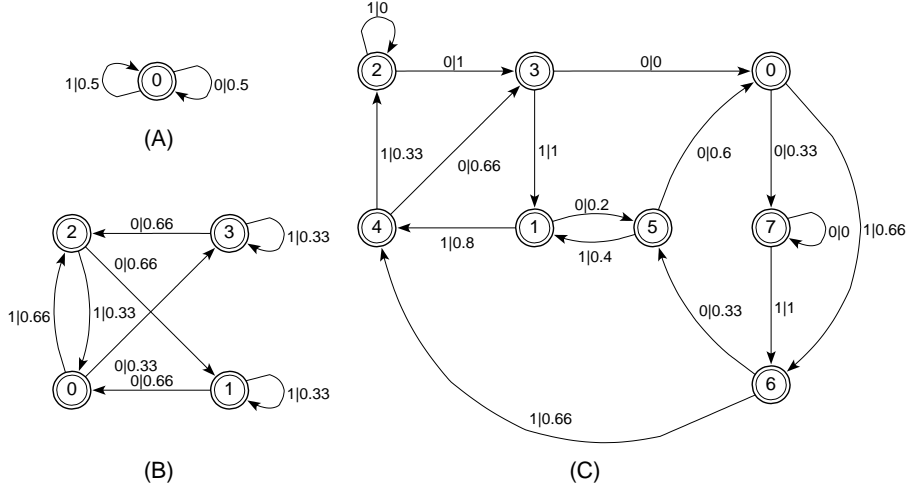


Figure 2: Examples of ε -machines. (A) ε -machine for a random fair coin. (B) ε -machine for the random-random-xor sequence. (C) ε -machine for random-negation-xor sequence.

part of the story. We are also interested in the computational structure behind the dynamics. We would expect to have some correlation between the computational complexity and the inherent information content of the system.

Here I will use the CSSR algorithm to ascertain the intrinsic computation of system under investigation. In general, in order to apply CSSR we need to know the orbit of a dynamical system (which we assume to be stationary process). As before we then take measurements of the change in state variables, as the system moves along its attractor. Given a data stream in the form of a long measurement sequence, the first step in the process (machine) reconstruction is the construction of a tree. A tree $T = \{n, l\}$ consists of a set $n = \{n_i\}$ nodes and a set of directed labeled arcs $l = \{l_i\}$ connecting them in a hierarchical structure with no circuits. An L -level subtree T_n^L at node n is a tree that starts at node n and contains all nodes that can be reached within L steps of a walk. To construct a tree from a measurement sequence we simply parse the stream for all length- l sequence and from this construct the tree with links up to level L that are labeled with individual symbols up to that time. We add a probabilistic structure to the tree by recording for each node n_i the number of $N_i(L)$ of occurrence of the associated sequence of symbols relative to the total number $N(L)$ of observations of length L $p_{n_i}^T(L) = \frac{N_i(L)}{N(L)}$. This gives a hierarchical approximation of the measure of the dynamics.

The ε -machines are represented by a class of labeled directed multi-graphs or l-digraphs and they are directly related to Shannon graphs of Information Theory (refs), and to discrete finite automata in computation theory. In the most general form we are concerned with a probabilistic version of these systems. Their topology is described by a digraph $G = \{V, E\}$ that consists of vertices $V = \{v_i\}$ and a set of edges $E = \{e_i\}$ connecting the vertices. Each arc carries a label $s \in \mathcal{A}$.

To reconstruct a topological ε amine we define an equivalence relation subtree similarity, denoted on the nodes of the tree by the condition that the L -subtrees are identical $n_i \approx n_j$ if and only if $T_{n_i}^L = T_{n_j}^L$. Subtree equivalence means that the link structure is identical. This equivalence relation induces a set of equivalence classes $\{C \mid l = 1, \dots, K\}$ given by $C \mid \{n \in N : n_i \in C \text{ and } n_i \in C \mid \text{iff } n_i \approx n_j\}$. We will refer to the archetypal subtree link structure for each class as a morph. A graph G_L is then constructed by associating a vertex to each tree node L -level equivalence class. Two vertices v_k and v_l are connected by a directed edge if the transition exists in the tree between nodes in the equivalence classes, $n_i \rightarrow n_j : n_i \in C_k^L, n_j \in C_l \mid$. The corresponding arc is labeled by the same symbol associated with the tree nodes in the equivalence classes.

In this way, ε -machine reconstruction deduces from the diversity of the individual temporal patterns from the signal a set of generalized states associated with the graph vertices that are optimal for forecasting. The topological ε -machine so reconstructed capture the essential computational aspects of the data stream by producing the simplest model to recreate the data stream.

As a practical demonstration of the ε -machine state space reconstruction algorithm figure 2 displays three machines derived from (A) a random sequence of 0's and 1's; (B) two random values either 0 or 1 followed by xor of the previous two digits; (C) random number, negation xor of the previous two digits.

3.3 Coding Population Fluctuations

To understand the statistical complexity of rock–paper–scissors, we need to know the orbit of the dynamical system. Let $\{f_t\}_{t=0}^n$ be a sequence of real valued numbers representing the population density of rock (n_r) at each time step. The sequence $\{f_t\}_{t=0}^n$ forms a time series that contains information about the orbit of the population around its attractor. We need to decompose the $\{f_t\}_{t=0}^n$ into an ensemble of objects that describe the course grain behavior of the game for a given parameter configuration. The ensemble can be defined as a string $S(\varepsilon) = s_1, s_2, \dots, s_n$ of symbols where $s_i \in \{\bar{1}, 0, 1\}$. $S(\varepsilon)$ is obtained from $\{f_t\}_{t=0}^n$ by $s_i = \Psi_{f_t}(i, \varepsilon)$ where:

$$\Psi_{f_t}(i, \varepsilon) = \begin{cases} \bar{1} & \text{if } f_i - f_{i-1} < -\varepsilon \\ 0 & \text{if } |f_i - f_{i-1}| \leq \varepsilon \\ 1 & \text{if } f_i - f_{i-1} > \varepsilon \end{cases}, \quad (11)$$

the signal or message $S(\varepsilon)$ contains course grain information about the rate of change of the rock population. The parameter ε , can be thought of as a filter, that that can be used to do dampen out low-level fluctuation in population density. Similarly, large values of ε can be used to only focus on the large population fluctuations.

3.4 Results

Time series data of population fluctuations for P_0 containing 300,000 time steps were constructed. P_0 was systematically varied in increments of 0.01 between 0 and $\frac{5}{6}$ (see §2). The function in equation 11, was then applied with $\varepsilon = 0$, so that all minor fluctuations were taken into account. Each time series was 2 million points in length. The information theory statistics and the CSSR algorithm outlined in section §3 were then applied to each of the time series.

3.4.1 Information Content, Memory and Randomness

For each of the time series, the *block entropy*, *source entropy*, *excess entropy* and *redundancy*, was calculated. Figure 3 illustrates the results of these calculations. Blocks lengths L of size 1, 2, 3, 4, 5, 10, 20, and 30, were used to analyze the complexity of the signals. The analysis reveals that for low values of P_0 the signal has a low complexity, but there is a large jump in the signal complexity when $P_0 \approx 0.08$. This indicates that the predictability of the population dynamics is at it's most unpredictable at this threshold. The longer the blocks L , the greater the accuracy in predicting system behavior.

3.4.2 Computational Complexity and Dynamics

For each of the time series, ε -machines were constructed using the method outlined in §3.2. The ε -machines are simple models that can generate a signal similar to that created by the complex system. Figure 4 illustrates four ε -machines, for $P_0 = 0, 0.03, 0.08$, and 0.77 . These machines show a change in the computational complexity of the signal. When $P_0 = 0$ the machine is a sink machine, the dynamics collapse to a fixed point from which it cannot escape. When $P_0 > 0$ the dynamics become a simple toggle machine which a bucket state that cannot be escaped from. For $0.08 < P_0 < 0.7$ the machine has a high computational complexity with both fast and slow dynamics representing the cyclic behavior. Finally when $P_0 > 0.7$ the machine reverts back to a toggle machine with a bucket state that can not be escaped from. Figure 4 plots these machines against their $h_\mu(1)$ and typical population dynamics. The relationship between these measures will be discussed in more detail in the following section.

3.5 Discussion

Figures 3 and 4 show four distinct regions. The first region occurs when $P_0 = 0.0$, this can be described as a *frozen state*. As P_0 is unable to invade P_1 , P_2 consumes all accessible P_0 , and P_1 drives P_2 to extinction. With P_0 unable to replace P_1 , the cycle is broken and P_0 and P_1 coexist in a frozen steady state. However when $P_0 > 0$, we move from the frozen co-existing state to a P_0 *dominant state*, again this is a fixed point or frozen state, where P_0 drives the other two players to extinction and dominates the entire lattice. The when $P_0 \approx 0.0798$ there is a transition form the P_0 dominant state to a complex dynamics. The ε -machine in figure 4 shows that a dynamic which fast and slow moving components. The population dynamics begin to oscillate cyclicly. At this point the information measures are maximized (see figure 3). The population dynamics at this point also have large oscillation and slow dampened oscillations. The final region I will refer to as P_0 dominated state, this occurs when the other species drive P_0 to extinction. This occurs when $P_0 \approx 0.7$, but this could be due to finite size effects. At this threshold, the population dynamics return to a fixed state, the dynamics can be reconstructed with a simple ε -machine, and the entropy measures indicate simple dynamics. In the next section I will investigate the

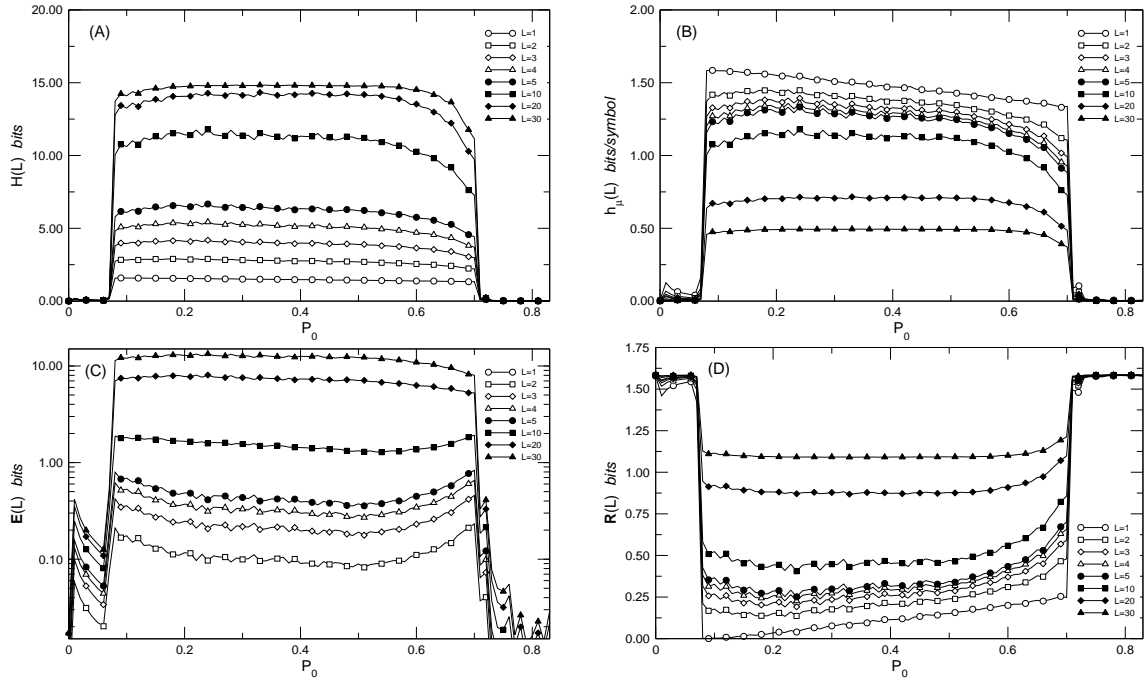


Figure 3: Statistical Complexity. These plots illustrate the complexity of the dynamics. (A) Block Entropy, shows the amount of information, or amount of memory within the system. As the blocks become longer, more and more information about the system behavior is captured. When $P_0 < 0.0798$, the system is highly predictable, and only short blocks are required to capture the behavior of the system. However when $P_0 > 0.0798$ the information content within the dynamics is increased dramatically. This transition behavior is also shown in (B) Source Entropy, (C) Excess Entropy and (D) Redundancy.

structure and change in structure of the P_0 population at the transition between *frozen state*, and the P_0 *dominant state*.

4 Percolation Properties

The previous section outline was able to characterize the orbit of the population fluctuations both in terms of information content and computational complexity of a dynamical system. I will now focus on the spatial structural characteristics of the system. Figure 4 showed that there are significant transitions in the behavior of the system at critical values of P_0 , in central question here is what major spatial structural changes occur to the population as P_0 increases. To do this we will introduce the percolation (Stauffer 1985) properties of the P_0 players.

Phase changes and criticality are common in biology. Examples include cell differentiation and vegetation change. Perhaps the most striking biological examples of criticality are epidemics. The spread of a disease, for instance, depends on its infection rate and if the connectivity is below a critical threshold then the epidemic dies out naturally; however if the population is above the critical threshold, then the epidemic spreads indefinitely. All epidemic processes exhibit phase changes. For instance, fire spread depends on a critical level of fuel density and invasions by exotic plants require landscapes that possess a critical density of sites available for colonization.

Percolation theory studies the emergence of such phenomena. More specifically percolation theory studies paths that percolate the lattice (starting at one side and ending at the opposite side). For small p only a few steps are possible, thus only small clusters of nodes connected by edges can form, but at a critical probability p_c , called the percolation threshold, a percolating cluster of nodes connected by edges appears (see figure 5). This cluster is also called the infinite cluster, because its size diverges as the size of the lattice increases. There are several much studied versions of percolation, the one presented above being “bond percolation”. The most known alternative is site percolation, in which all bonds are present and the nodes of the lattice are occupied with probability p . In a similar way as bond percolation, for small p only finite clusters of occupied nodes are present, but for $p > p_c$ an infinite cluster appears. Figure 6 illustrates this point. When the concentration of occupied cells is below the critical level p_c the occupied cells exist as a sequence of disconnected clusters (figure 6 right). At the critical value it is unknown if an infinite cluster exists (figure 6 center). Finally if $p > p_c$ then the system contains an infinite cluster.

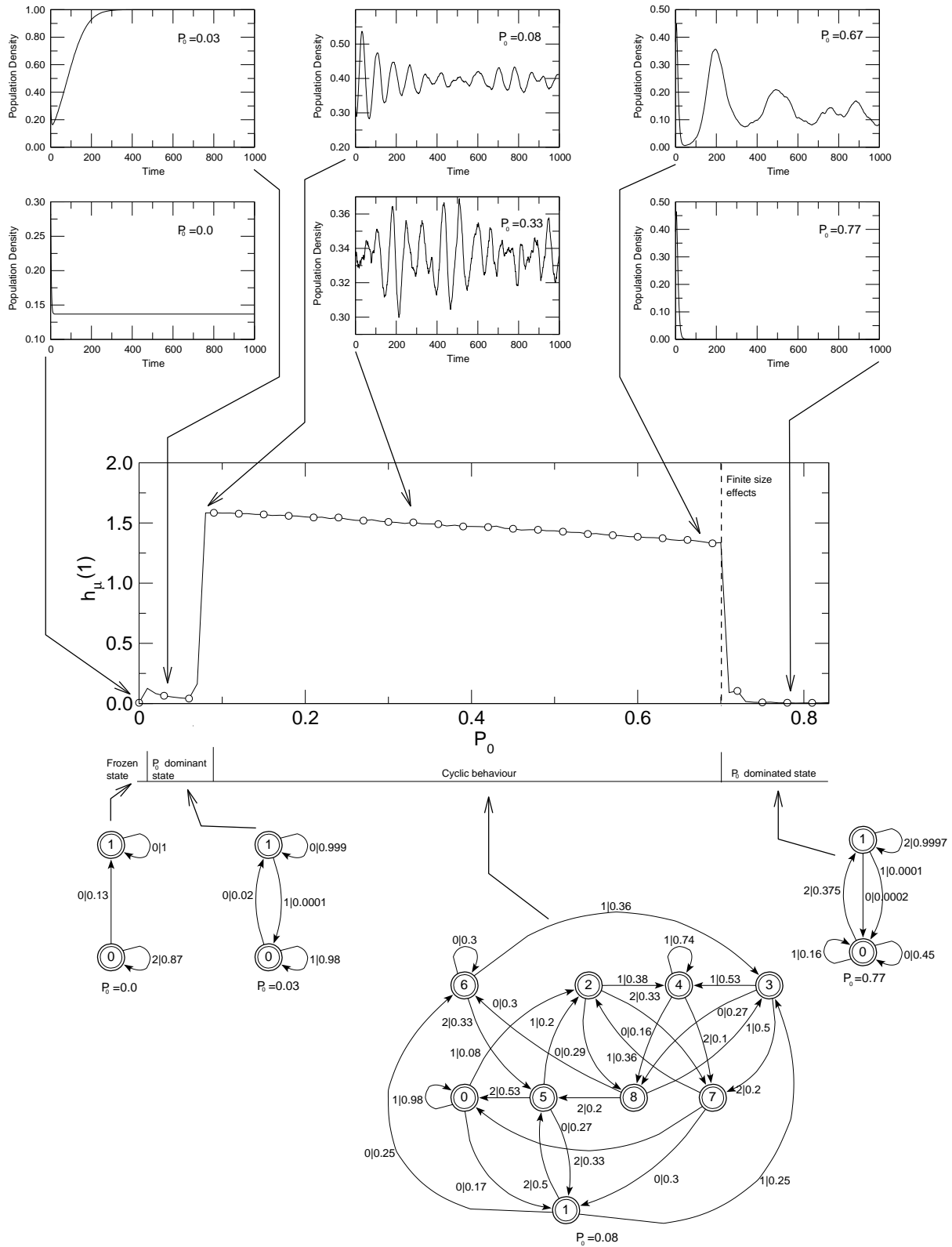


Figure 4: Computational Complexity of Rock-Paper-Scissors. This figure shows the relationship between the raw time-series data, h_{μ} , and ε -machines, for selected points along the parameter space transect. The parameter transect can be divided into four distinct behaviors. First when $P_0 = 0$, the system freezes into a static configuration, where two species coexist. The second state is also a steady state, where P_0 dominates other species. The third state contains complex and chaotic dynamics. Finally the fourth state is a steady state where P_0 becomes extinct.

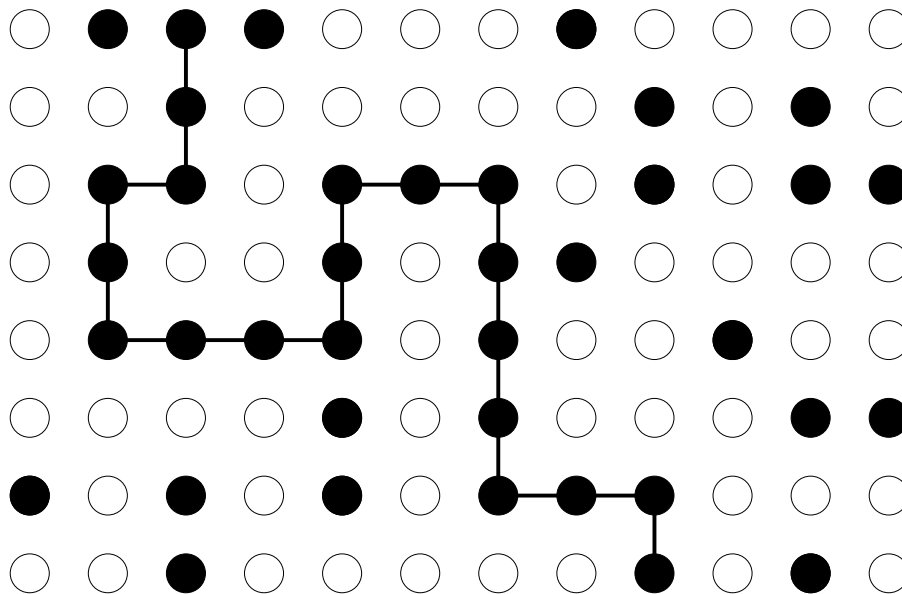


Figure 5: Example of the shortest path connecting the top of a small square lattice with the bottom for p slightly above p_c .

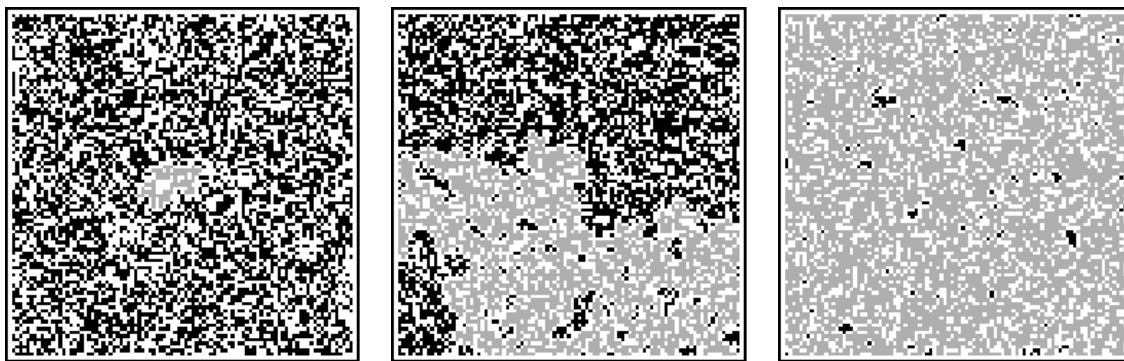


Figure 6: Criticality phenomena in percolation model. (Left) Example of a percolation lattice where with probability of a site being occupied is set to 0.5. Under this scheme the occupied sites exist as a series of disconnected clusters (Cluster marked in gray). (Centre) Example of a percolation lattice where with probability of a site being occupied is set to 0.6. Near the critical threshold the occupied sites form clusters of all possible sizes (Again a large cluster is marked in gray). At this point there may exist an infinite cluster that spans the lattice. (Right) Example of a percolation lattice where with probability of a site being occupied is set to 0.7. Here the occupied sites form an infinite cluster that spans the lattice (Giant cluster marked in gray).

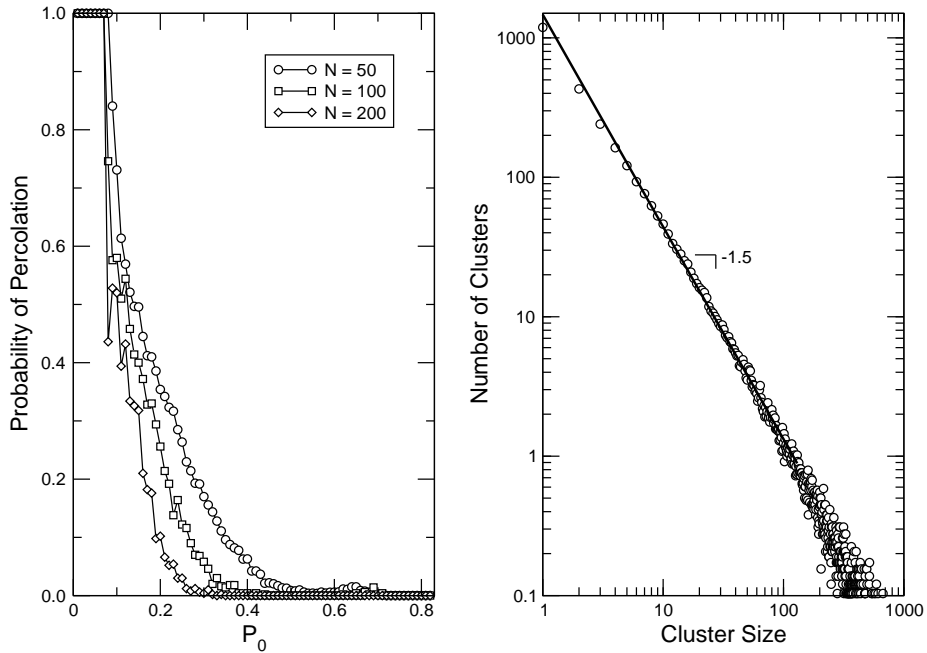


Figure 7: This is the caption (Right) Monte carlo data for the size and frequency of cluster sizes.

Percolation processes are commonly studied in statistical physics. The two major questions of interested in any percolation system under investigation is: (1) Does there exist a giant component that spans the lattice and what are the critical values for the emergence of such a cluster; and (2) What are the structural characteristics of the giant cluster. The following sections will examine these questions in turn.

4.1 Percolation Threshold

One of the most interesting findings of random graph theory is the existence of a critical probability at which a giant cluster forms. Translated into network language, it indicates the existence of a critical probability p_c such that below p_c the network is composed of isolated clusters but above p_c a giant cluster spans the entire lattice. This phenomenon is similar to transition phenomena commonly studied in mathematics and in statistical mechanics (Stauffer 1985). To determine if an infinite cluster exists, I constructed lattices of size 50×50 , 100×100 , 200×200 , 300×300 , 400×400 and 500×500 . The game was played out for 1,000 time steps and the lattice was checked for the existence of cluster of rock players that spanned the entire lattice. This was repeated 1,000 times for each value of P_0 . Figure 7 illustrates the results of the experiment. Figure 7 Right show that a giant cluster exists for $0 < P_0 < 0.8$. More detailed analysis reveals that the giant component breaks down at $P_0^{critical} \approx 0.0798$. For values larger than this, the lattice does not contain a giant cluster of rock players.

At the critical point, Figure 7, shows the frequency distribution of clusters. This plot forms a power law with a slop of -1.5 . This suggests that the at the critical point the game of Rock–paper–scissors is not self-organizing critical (Bak 1996).

4.2 Cluster Structure at the Critical Point

Much of the interest in the properties of dilute systems is in their geometrical structure near the critical percolation threshold p_c . Studying the structure is clearly the first step in understanding the physical properties of the system (e.g. the ability a species has to invade another species). Generally the properties of a system depend on the structure of the infinite cluster. For the system considered here, this is when $P_0 \approx p_c$. Where P_c is the percolation cluster. In percolation studies the probability of belonging to this cluster is $P_\infty(p) \approx (p - p_c)^\beta$, and the correlation length is $\xi \approx |p - p_c|^{-\nu}$ (Stauffer 1985). On length scales which are long compared to ξ , the cluster occupiers

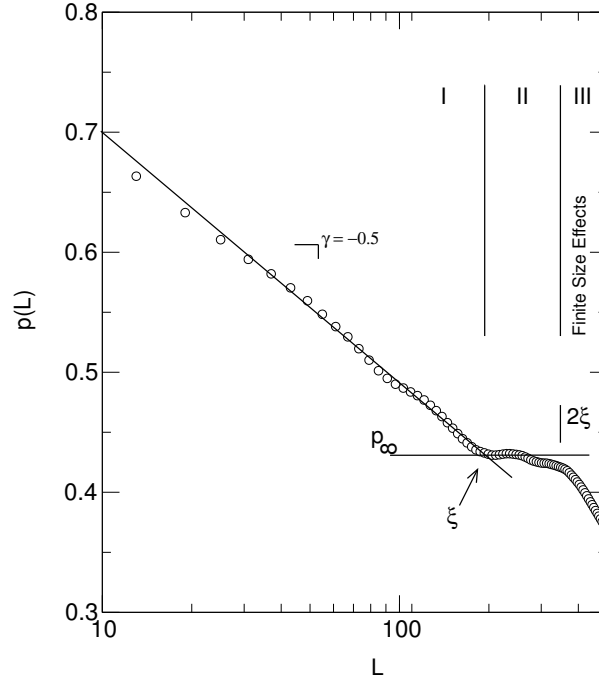


Figure 8: Cluster Mass Analysis. The analysis of the structure of the cluster reveals that as L increases, there are three distinct regions. Region I the cluster mass to volume ratio displays power-law scaling. Region II shows the constant growth of the cluster. The intersection of regions I and II indicate the critical length-scale ξ . Region III shows a decline in cluster grown, this is likely to be due to finite size effects.

some homogeneous space. On smaller scales, the correlations create fluctuations in the density. These fluctuations create self-similar properties.

Self-similarity is intimately linked to with the notion of fractal dimensionality (Mandelbrot 1977). There has been numerous attempts to characterize the fractal dimensionality of the largest finite cluster generated through a percolation processes (such as the one studied here) (Stauffer 1985). In contrast to the various finite scaling arguments, I follow a the geometrical procedure proposed by Mandelbrot (1977). Given a point on the infinite cluster consider the number $M(L)$ of points on the same cluster with a volume L^d (of linear size L) centered at that point. Self-similarity implies that the $M(L)$ scales as

$$M(L) = L^D, \quad a \ll L \ll \xi, \quad (12)$$

where D is the fractional dimensionality. In the remainder of this section I will use a Monte Carlo simulation to explore the self-similarity properties of the infinite cluster near the critical exponent. For the critical value of P_0 I generated 10,000 samples of 501×501 games of rock-paper-scissors. Those samples that contained an infinite cluster, and contained a P_0 player as part of the giant cluster at the center of the lattice were kept for analysis. This was about 1,000 cases. Once a sample was identified, sites connected to the giant cluster and occupied by P_0 players were counted in boxes of size L , giving the volume $M(L)$. Averaging over these samples, I found the average density $p(L) = M(L)/L^2$. Figure 8 shows a typical plot for $P_0 = 0.0798$. Similar plots were found for other values of P_0 near the critical point.

Figure 8 exhibits three distinct regions: Region I, indicates a power law behavior, $p(L) \approx L^\gamma$ ($\gamma = 2 - D = 0.5$). Region II, depicts a constant growth in the cluster size, the intersection between these two regions in the point where $L = \xi$, that is when L is equal to the critical length ξ . Region III is the result of finite size effects.

Figure 8 demonstrates that although $P(p)$ is the average probability of an occupied site to be on the infinite cluster at length L is not uniform for $L < \xi$. Further analysis of the structure requires the system to be divided into “boxes” for $L < \xi$ and $L > \xi$.

The experiments in this section have shown the giant cluster formed by a P_0 at the critical threshold displays self-similarity. The onset of the breakdown of the giant cluster, coincides with the emergence of complex behavior. From figure 4 we see that at this critical point, predictability is decreased, and the computational complexity increases. The fractal nature of the giant component at this point is a contributing factor in the complex dynamics, as stochastic epidemic processes (such as a random walk) require maximum time to fill such clusters.

5 Discussion

An important aspect of large-scale connectivity is communication between sites and regions within a landscape. For plants, local communication occurs by seed dispersal, which leads to clumped distributions and plays a key role in maintaining high species diversity. Dispersal is also essential to maintain genetic homogeneity within populations. Should the connectivity between sites provided by dispersal fall below a critical level, then a regional population effectively breaks up into isolated sub-populations. So a decrease in gene flow could suffice for speciation to occur, even in the absence of major landscape barriers. In this study I have examined the affect of spatial constraints on successional system. The major points from this study can be summarized as:

- The mean field equations demonstrate the “survival of the weakest” phenomena. When spatial constraints are introduced into the model, global extinction is unlikely to occur, sub-populations are likely to persist, and population densities fluctuate;
- Treating the model as an information source, and the population densities as a signal, the use of information theoretic measures have been able to characterize the dynamics of the system in terms of excess entropy, intrinsic memory, regularities, randomness and redundancy;
- The information theoretical analysis demonstrated there were four distinct system behaviors along the studied transect:
 1. A frozen co-existing state. This occurred when $P_0 = 0.0$. Essentially P_2 becomes extinct and with P_0 unable to invade P_1 the two species co-exist in a frozen state;
 2. A frozen P_0 dominant state. This occurs when $0 < P_0 < 0.0798$. P_0 displays the survival of the weakest phenomena and out competes the other two species;
 3. Complex cyclic state. This occurs when $0.0798 < P_0 < 0.7$. In this state the population densities oscillate; and
 4. A frozen state where P_0 becomes extinct. This occurs when $P_0 > 0.7$. P_0 is too competitive and is out competed by its competitors.
- The use of a state space reconstruction algorithm the ε -machine, has been able to develop finite state machines which capture the computational complexity of the behavior of the population dynamics. Again there is a quantitative change in the structure, complexity and nature of the machines in alignment with states identified by the information theory measures;
- Analysis of the size of the giant component of P_0 players, indicates that the onset of the complex behavior coincides with the breakdown of a cluster which spans the entire lattice; and
- Analysis of the structure of the giant connected component at point where it breaks down shows that it is self-similar and displays fractal properties.

Notions of resource competition lead to ideas of competitive exclusion that state complete competitors cannot coexist (Harding 1960). Those species most well adapted to an environment are most likely to capture a larger share of the available resources. Every improvement in one species will lead to a selective advantage for that species over another. However, since in general different species are co-evolving, improvements in one species implies that it will get a competitive advantage on the other species, and thus be able to capture a larger share of the resources available to all. This means that fitness increase in one evolutionary system will tend to lead to fitness decrease in another system. The only way that a species involved in a competition can maintain its fitness relative to the others is by in turn improving its design. This is known as the Red Queen effect, and was proposed by van Valen (1973), and is based on the observation to Alice by the Red Queen in Lewis Carroll’s book *Through the Looking Glass*; that “*in this place it takes all the running you can do, to keep in the same place.*” The study here only examined static populations. An interesting further study would be to examine how the dynamics of the systems change when natural selection is allowed to design the strategies of the individual players.

ACKNOWLEDGEMENTS

The author would like to thank Ian G. Enting for a number of useful discussions about the percolation properties of Rock–paper–scissors. The author would also like to thank John Finnigan, Markus Brede, and Fabio Boschetti, for a number of useful discussions about this paper and the methods present within it.

References

- Bak, P. (1996). *How nature works*. Springer-Verlag.
- Burrows, M. T. & Hawkins, S. J. (1998). "Modelling patch dynamics on rocky shores using deterministic cellular automata" *Marine Ecology Progress Series*. **167**: 1–30.
- Buss, L. W. (1980). "Competitive intransitivity and size-frequency distributions of interacting populations" *Proceedings of the National Academy of Science*. **77**: 5355–5359.
- Crutchfield, J. P. & Feldman, D. P. (2003). "Regularities unseen, randomness observed: Levels of entropy convergence." *Chaos*. **13**: 25–54.
- Crutchfield, J. P. & Young, K. (1989). "Inferring Statistical Complexity" *Physical Review Letters*. **163**(2): 105–108.
- Frean, F. & Abraham, E. R. (2001). "Rock–scissors–paper and the survival of the weakest." *Proceedings of the Royal Society London Series B*. **268**: 1323–1327.
- Haken, H. (1998). "Information and Self-Organisation" *Springer Series in Synergetics*. **40**.
- Johnson, C. R. (1997). "Self-organising in spatial competition systems" *Frontiers in ecology—building the links*. pp. 245–263.
- Mandelbrot, B. B. (1977). *Fractals, form, chance, and dimension*. W.H. Freeman and Co.. San Francisco, California.
- Shannon, C. E. (1948). "A mathematical theory of communication" *Bell Sys. Tech. J.* **27**: 379–423.
- Sigmund, K. (1993). *Games of life: explorations in ecology, evolution and behavior*. Oxford University Press.
- Sinervo, B. & Linely, C. M. (1996). "The rock–paper–scissors game and the evolution of alternative male strategies" *Nature*. **380**: 240–243.
- Stauffer, D. (1985). *Introduction to Percolation Theory*. Taylor and Francis.
- Valen, L. V. (1973). "A New Evolutionary Law" *Evolutionary Theory*. **1**: 1–13.